Experimental Failure Analysis of Two-Serial-Bolted Composite Plates

Faruk Sen,[1] Onur Sayman[2]

[1]*Department of Mechanical Engineering, Aksaray University, Aksaray, Turkey*
[2]*Department of Mechanical Engineering, Dokuz Eylul University, Bornova, Izmir, Turkey*

Received 5 April 2008; accepted 20 January 2009
DOI 10.1002/app.30118
Published online 19 March 2009 in Wiley InterScience (www.interscience.wiley.com).

ABSTRACT: In this study, a failure analysis of two-serial-bolted glass-fiber-reinforced epoxy composite plates was performed. To determine the influences of the joint geometry and stacking sequences on the bearing strength and failure mode, parametric studies were carried out experimentally. Three different geometrical parameters—the ratio of the edge distance to the hole diameter (E/D), the ratio of the plate width to the hole diameter (W/D), and the ratio of the distance between two holes to the hole diameter (K/D)—were considered. For this reason, the E/D, W/D, and K/D ratios were designed to range from 1 to 5, from 2 to 5, and from 3 to 5, respectively. Furthermore, the tests were performed with various preload moments (2, 3, 4, and 5 Nm) and without any preload moments (0 Nm). Because of the observed effect of the material parameters on the failure behavior, composite laminated plates were stacked in two different stacking sequences: $[0^\circ/0^\circ/30^\circ/30^\circ]_s$ and $[0^\circ/0^\circ/45^\circ/45^\circ]_s$. The experimental results indicated that the failure response of the two-serial-bolted joints were strictly affected by the material parameters, geometrical parameters, and values of the applied preload moments. © 2009 Wiley Periodicals, Inc. J Appl Polym Sci 113: 502–515, 2009

Key words: composites; failure; fibers

INTRODUCTION

Fiber-reinforced composite materials have been widely used in aircraft and space structures because of their high specific modulus and high specific strength. Because the use of composites has become popular in recent years, the construction of composite joints has become a very important research area as the structural efficiency of a composite structure is determined by its joints, not by its basic structures.[1] Bolts, pins, and rivets have been used widely in these applications for transferring load between the structural components.[2] Among the different techniques for joining structural parts, mechanical fastening through a pin or bolt is a general choice because of the low cost, simplicity, and ease of disassembly for repar.[3] On the other hand, for structural components that must be removed or easily replaced, mechanical fasteners play an important role.[4] Nevertheless, bolted joints require holes to be drilled in the structure, and large stress concentrations tend to develop around the holes and can severely reduce the overall strength of the structure.[5] Unlike many metallic structural parts, for which the strength of the joints is mainly governed by the shear and tensile strengths of the pins or bolts, composite joints present specific failure modes because of their heterogeneity and anisotropy.[6]

Madenci et al.[7] developed an analytical methodology, based on the boundary collocation technique, to determine the contact stresses and stress intensity factors required for strength and life prediction of bolted joints with many fasteners. It provides an analytical capability for determining the contact stresses in mechanically fastened composite laminates while capturing the effects of the finite geometry, presence of edge cracks, interactions among fasteners, material anisotropy, fastener flexibility, fastener-hole clearance, friction between the pin and the laminate, and bypass loading. McCarthy et al.[8] investigated the effects of bolt-hole clearance on the load distribution and failure mechanisms of multi-bolt, double-lap composite joints using three-dimensional finite element analysis coupled with a progressive damage model. Contact between each bolt and hole was included in the analysis. The results were compared with an experimental study in which joints were instrumented to obtain the load distribution and loaded to ultimate failure. An experimental study was performed to assess the effects of clamp-up on the net tension failure of laminated composite plates with bolt-filled holes.[9] The tensile strength and failure response of specimens with an open hole and a bolt-filled hole were evaluated. Experimental results showed that the bolt clamping force could significantly reduce the notch

Correspondence to: F. Sen (faruk.sen@deu.edu.tr).

© 2009 Wiley Periodicals, Inc.

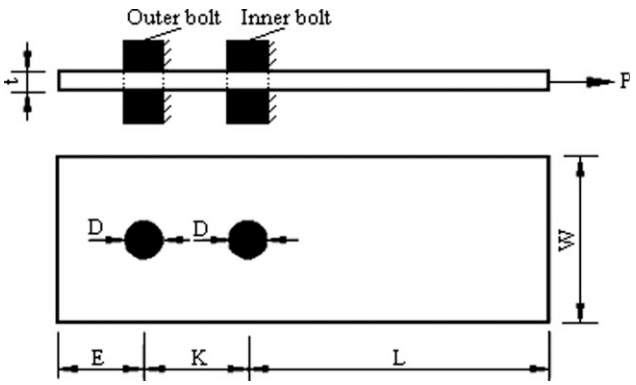

Figure 1 Dimensions of a laminated composite plate with two serial bolts.

tensile strength of composite laminates, which were prone to fiber–matrix splitting and delamination. Higher clamping pressure resulted in higher reductions of the notch strength. Tong[10] experimentally investigated the effect of nonuniform bolt-to-washer radial clearance on the bearing failure of bolted joints under different clamping forces with various lateral constraints. The experimental results were also used to validate an existing model. Two extreme diametral fit positions, with a positive or negative bolt-hole-to-washer clearance, were also examined. Lin and Lin[11] investigated stresses around a pin-loaded hole in symmetrically stacked composite laminates of finite size using a two-dimensional direct boundary element method. Effects of friction and clearance between the pin and hole edge on the stresses were obtained because geometric compatibility and force constraint between the pin and the plate were enforced.

Meola et al.[12] experimentally investigated an innovative glare fiber-reinforced metal laminate with the aim of characterizing its strength and behavior in the case of mechanical joints. Several specimens were fabricated through the variation of the width and hole-to-edge distance and tested in a pin-bearing fashion without lateral restraints; this was the most critical testing procedure for the simulation of mechanical joints. Specimens, after bearing stress, were analyzed in both nondestructive and destructive ways. Okutan[13] performed a numerical and experimental study to observe the failure behavior of mechanically fastened fiber-reinforced laminated composite joints. Tests were carried out on single pinned joints in $[0/90/0]_s$ and $[90/0/90]_s$ laminated composites. Furthermore, a method was presented for predicting the failure strength and failure mode of mechanically fastened fiber-reinforced composite laminates by Chang et al.[14] A computer code was developed that could be used to calculate the maximum load and mode of failure of joints involving laminates with different ply orientations, different material properties, and different geometries. Parametric studies were also performed to evaluate the effects of the joint geometry and ply orientation on the failure strength and on the failure mode. Pakdil et al.[15] investigated the effect of preload moments on the failure response of glass–epoxy-laminated composite single-bolted joints with bolt/hole clearance. To evaluate the effects of the bolted-joint geometry and stacking sequence of laminated plates on the bearing strength and failure mode, parametric analysis was performed experimentally. Additionally, Sayman et al.[16] conducted a failure analysis to determine the bearing strengths of mechanically fastened joints with single bolts in glass–epoxy-laminated composite plates.

In this study, an experimental failure analysis was carried out to determine the failure behavior of two-serial-bolted glass-fiber-reinforced epoxy composite plates. The analysis was performed experimentally. Tests were applied both with various preload moments and without preload moments. In addition, the effects of the stacking sequences and a variety of geometrical parameters of the composite specimens on the failure response and bearing strengths were considered.

EXPERIMENTAL

In this study, laminated composite rectangular specimens (length L, width W, and thickness t), produced from glass-fiber-reinforced epoxy unidirectional plies with two circular holes filled with two rigid steel bolts, were used. The dimensions of the composite specimens are illustrated in Figure 1. Hole diameter D was fixed at a constant value of 5 mm. The outer hole was located along the centerline of the plate at distance E from one end of the plate. Moreover, the inner hole was positioned at distance K from the center point of the outer hole. Consequently, the ratios of the edge distance to the hole diameter

TABLE I
Stacking Sequences and Selected Parameters of the Tested Composite Specimens

Stacking sequence	t (mm)	D (mm)	E/D	W/D	K/D	Total number of laminas
$[0°/0°/30°/30°]_s$	1.6	5	1, 2, 3, 4, 5	2, 3, 4, 5	3, 4, 5	8
$[0°/0°/45°/45°]_s$	1.6	5	1, 2, 3, 4, 5	2, 3, 4, 5	3, 4, 5	8

TABLE II
Mechanical Properties of the Glass Fiber/Epoxy-Laminated Composite Material

Material properties	Symbol	Units	Values
Fiber volume fraction	V_f	%	59
Longitudinal modulus	E_1	MPa	43500
Transverse modulus	E_2	MPa	16250
Shear modulus	G_{12}	MPa	6970
Poission's ratio	v_f	MPa	0.28
Longitudinal tension	X_t	MPa	940
Longitudinal compression	X_c	MPa	940
Transverse tension	Y_t	MPa	109
Transverse compression	Y_c	MPa	156
Shear strength	S	MPa	91

(E/D) were selected to be 1, 2, 3, 4, and 5. The ratios of the specimen width to the hole diameter (W/D) were chosen to be 2, 3, 4, and 5. Furthermore, the ratios of the distance between two serial holes to the hole diameter (K/D) were chosen to be 3, 4, and 5. Hence, the form of each specimen was a rectangular strip of laminate of constant thickness t (1.6 mm) and width W, and the total length ($L + K + E$) of each specimen was 135 mm, with the 0° ply fiber axis parallel to the length. Composite laminated plates were stacked in two different stacking sequences—$[0°/0°/30°/30°]_s$ and $[0°/0°/45°/45°]_s$—symmetrically. The stacking sequences and selected parameters of the tested composite specimens are summarized in Table I. A uniform tensile load (P) was applied to each specimen, and the rigid bolts, supported outside the plate, resisted this load. The applied tensile load was also parallel to the laminate, and it was symmetric with respect to the centerline. Therefore, the applied load could not create bending moments about the x, y, and z axes.

The laminated composite plates used in the experiments were produced at Izoreel Firm (Izmir, Turkey). Two different laminate configurations were selected so that the significance of the fiber orientation and interaction effects of mixed fiber orientations on the strength could be investigated. Moreover, the selection of these lay-ups was used to examine a variety of failure modes and bearing strengths. All laminated plates were balanced about the midplane both to prevent thermal distortion for the period of production and to eliminate twisting and bending under tension. All composite plates were produced with E-glass fiber and an epoxy resin with a press-mold technique. Additionally, for the matrix material, epoxy CY225 and hardener HY225 were mixed in the mass ratio of 100 : 80. The epoxy resin and hardener mix was applied to the glass fibers. Then, the fibers were coated with this mix. Next, plies were placed one upon another as required by the stacking sequence. A hand roller was used to compact plies and take away entrapped air that could later lead to voids or layer separation. During the manufacturing process, the mold and lay-up were covered with a release material. Once the matrix material and fibers were combined, it was necessary to apply the proper temperature and pressure for specific periods of time to manufacture the fiber-reinforced laminated composite plate. Therefore, resin-impregnated fibers were positioned in the mold for curing. The press generated the pressure and temperature required for curing. Then, the mold was closed to give the nominal thickness. The glass fiber/epoxy material was cured at 120°C under a pressure of 9 MPa. After this, the temperature was held constant for 4 h for the first phase. Next, the temperature was decreased to 100°C and held constant for 2 h for the second phase. After the second phase, the laminates were cooled to room temperature. Finally, the laminated composite plate was removed from the press and cut to the specimen dimensions, as shown in Figure 1. The mechanical properties of this composite material were measured with an Instron 1114 test machine in the Mechanical Testing and Investigating Laboratory of the Mechanical Engineering Department at Dokuz Eylül University. Certain experiments were carried out to determine the mechanical properties, as described in refs. 15–20. The measured mechanical properties are presented in Table II.[20] In addition, on the basis of an in-plane assumption, the number of experiments required to describe the material parameters were reduced. Furthermore, during the determination of the mechanical properties, defining the coordinate system was very important. Therefore, a schematic view of a unidirectional fiber-reinforced lamina with global and material coordinate systems is illustrated in Figure 2.[21]

The failure tests were carried out in tension mode on the Instron 1114 test machine (with a 20-kN capacity), which was equipped with a chart to record the load–displacement curve of the specimen. A double-lap, two-steel-bolt joint was considered the experimental setup. The end of the specimen was

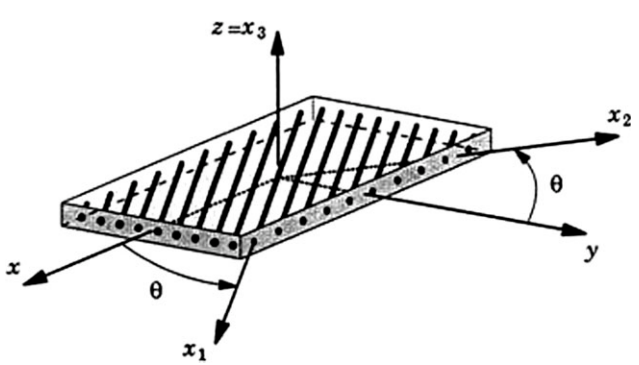

Figure 2 Definition of the global and material coordinate systems for a lamina.[21]

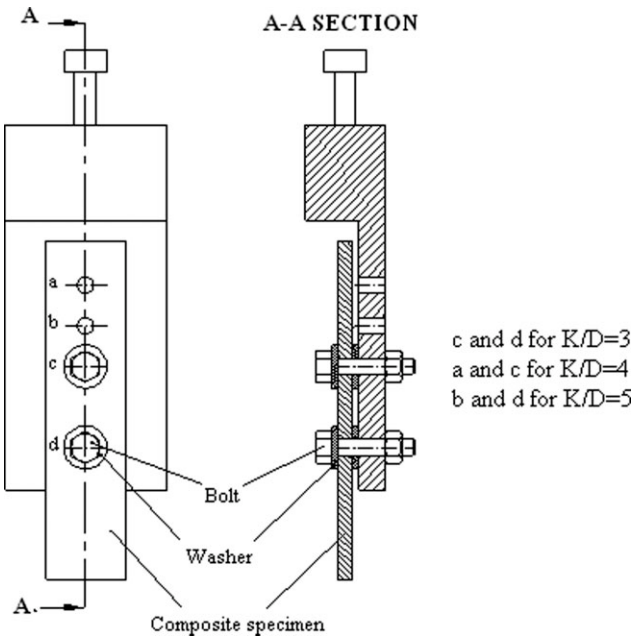

Figure 3 Two-serial-bolted joint test fixture (for $K/D = 3$).

positioned in wedge grips. The steel bolts were placed into the serial holes of the specimen. The other end of the specimen passed through a specially produced fork fitting connected to the test machine crosshead, as illustrated schematically in Figure 3. The curves of the load versus the bolt displacement for all composite configurations were drawn with a computer connected to the test machine. The tests were first carried out without any preload moments (0 Nm). Then, tests were performed for each designed specimen with a variety of preload moments applied (2, 3, 4, and 5 Nm). The main purpose of this was to determine the suitable value of the preload moment for a safety design with a two-serial-bolted composite joint. During the experiments, most testing was discontinued after two or three drops in the load were observed. The failure load was taken to be the first drop in the load and was related to the first appearance of cracking around the holes. A number of test specimens were tested to final failure. It was of interest to know to what extent damage had spread before the final failure load, and it was observed how failure was affected by geometrical parameters, especially the variation of the plate width and hole location.

Failure modes of bolted joints in laminated composite plates under tensile loads generally can be divided into four basic types: cleavage, net tension, shear-out, and bearing.[13–17] A schematic illustration of these failure modes is shown in Figure 4. Moreover, combinations of these failure modes are possible in practical applications. The main disadvantage of bolted joints is the formation of high stress concentration zones at the locations of the bolt holes, which might lead to a premature failure of the joint because of these failure modes or their combinations.[22]

RESULTS AND DISCUSSION

After the failure tests, the full number of tested specimens was equal to 900 for each stacking sequence because every similar type of specimen was tested three times for the determination of the average failure behavior and bearing strengths. Failure modes of every tested specimen were determined to investigate these three damaged specimens, and their load–displacement curves were plotted during the tests. The failure modes of whole tested $[0°/0°/30°/30°]_s$ and $[0°/0°/45°/45°]_s$ specimens are listed in Tables III and IV, respectively. According to these tables, the four different failure modes are cleavage, net tension, shear-out, and bearing. A schematic illustration of these failure modes is shown in Figure 4, as mentioned previously. The failure modes in inner and outer holes were similar for a number of tested specimens, such as bearing/bearing when W/D, E/D, and K/D were 5. Nonetheless, they were observed to be different for each hole, such as bearing/cleavage for $M = 0$ or net tension/cleavage for $M = 2$, 3, 4, or 5 when W/D was 2, E/D was 1, and K/D was 3. Moreover, combinations of these failure modes were observed for inner and/or outer holes of a quantity of tested specimens, such as bearing cleavage/shear-out, bearing net tension/bearing, and bearing cleavage/bearing cleavage, as shown in Tables III and IV. Some previous studies pointed out that combinations of failure modes are also possible.[13–17] The net tension and/or cleavage failure modes were observed when W/D was 2 for all E/D and K/D ratios. When W/D was 3, 4, or 5, the net tension and cleavage modes occurred after the bearing failure mode as part of mixed modes. Furthermore, no failure modes were observed in the outer hole when W/D was 2 because the net tension failure mode was created in the inner hole. It is known that the failure mode is catastrophic. Therefore, the

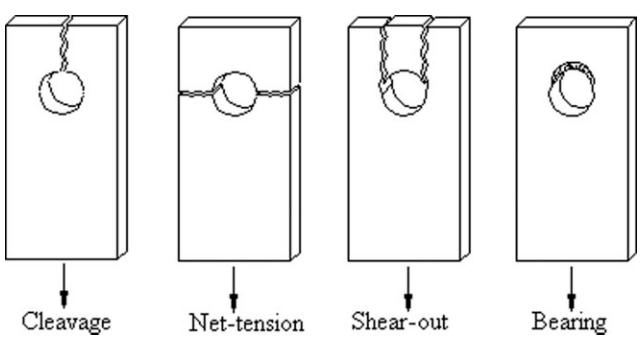

Figure 4 Common failure modes in bolted composite plates.

TABLE III
Failure Modes of $[0^\circ/0^\circ/30^\circ/30^\circ]_s$ Specimens

			Preload moments (inner/outer)				
W/D	*E/D*	*K/D*	0 Nm	2 Nm	3 Nm	4 Nm	5 Nm
2	1	3	B/C	N/C	N/C	N/C	N/C
		4	B/C	BN/C	BN/—	N/—	N/—
		5	B/C	BN/C	BN/C	N/C	N/C
	2	3	B/B	N/—	BN/—	N/—	N/—
		4	BN/B	N/—	BN/—	N/—	N/—
		5	BN/B	BN/—	BN/—	N/—	N/—
	3	3	BN/B	BN/—	BN/—	N/—	N/—
		4	BN/B	BN/—	BN/—	N/—	N/—
		5	BN/B	BN/—	BN/—	BN/—	BN/—
	4	3	BN/B	BN/—	BN/—	BN/—	BN/—
		4	BN/B	BN/—	BN/—	BN/—	BN/—
		5	BN/B	BN/B	BN/—	BN/—	BN/—
	5	3	BN/B	BN/B	BN/—	BN/—	BN/—
		4	BN/B	BN/B	BN/B	BN/—	BN/—
		5	BN/B	BN/B	BN/B	BN/—	BN/—
3	1	3	B/S	BC/S	B/S	BC/S	BC/S
		4	B/S	B/S	B/S	B/S	BN/C
		5	B/S	B/S	B/S	B/S	BN/S
	2	3	B/B	BN/B	BN/B	BN/B	BN/—
		4	B/B	BN/B	BN/B	BN/B	BN/—
		5	B/B	BN/B	BN/B	BN/B	BN/—
	3	3	B/B	BN/B	BN/B	BN/B	BN/—
		4	B/B	BN/B	BN/B	BN/B	BN/—
		5	B/B	BN/B	BN/B	BN/B	BN/B
	4	3	B/B	BN/B	BN/B	BN/B	BN/B
		4	B/B	BN/B	BN/B	BN/B	BN/B
		5	B/B	BN/B	BN/B	BN/B	BN/B
	5	3	B/B	BN/B	BN/B	BN/B	BN/B
		4	B/B	BN/B	BN/B	BN/B	BN/B
		5	B/B	BN/B	BN/B	BN/B	BN/B
4	1	3	B/S	BC/S	BC/S	BC/S	BC/S
		4	B/S	BC/S	BC/S	BC/S	BC/S
		5	B/S	B/S	B/S	B/S	B/S
	2	3	B/B	BC/BC	BC/BC	BC/BC	BC/BC
		4	B/B	BC/BC	BC/BC	BC/BC	BC/BC
		5	B/B	BC/BC	BC/BC	BC/BC	BC/BC
	3	3	B/B	BC/BC	BC/B	BC/BC	BC/BC
		4	B/B	BC/B	BC/B	BC/BC	BN/B
		5	B/B	BN/B	BN/B	BN/BC	BN/B
	4	3	B/B	BC/B	BC/B	BC/B	BN/B
		4	B/B	BC/B	BC/B	BC/B	BC/B
		5	B/B	B/B	BC/B	BC/B	BC/B
	5	3	B/B	BC/B	BC/B	BC/B	BC/B
		4	B/B	BC/B	BC/B	BC/B	BC/B
		5	B/B	BN/B	BC/B	BC/B	BC/B
5	1	3	B/S	BC/S	BC/S	BC/S	BC/S
		4	B/S	B/S	B/S	BC/S	BC/S
		5	B/S	B/S	B/S	B/S	B/S
	2	3	B/B	BC/BC	BC/BC	BC/BC	BC/BC
		4	B/B	BC/BC	BC/BC	BC/BC	BC/BC
		5	B/B	BC/BC	BC/BC	BC/BC	BC/BC
	3	3	B/B	BC/BC	BC/BC	BC/BC	BC/BC
		4	B/B	BC/BC	BC/BC	BC/BC	BC/BC
		5	B/B	BC/BC	BC/BC	BC/BC	BC/BC
	4	3	B/B	BC/B	BC/B	BC/B	BC/BC
		4	B/B	B/B	B/B	B/B	BC/BC
		5	B/B	B/B	B/B	B/B	B/B
	5	3	B/B	B/B	B/B	B/B	B/B
		4	B/B	B/B	B/B	B/B	B/B
		5	B/B	B/B	B/B	B/B	B/B

B = bearing; BC = bearing cleavage; BN = bearing net tension; C = cleavage; N = net tension; S = shear-out.

TABLE IV
Failure Modes of $[0^\circ/0^\circ/45^\circ/45^\circ]_s$ Specimens

			Preload moments (inner/outer)				
W/D	*E/D*	*K/D*	0 Nm	2 Nm	3 Nm	4 Nm	5 Nm
2	1	3	B/C	N/C	N/C	N/C	N/C
		4	B/C	N/C	N/C	N/C	N/C
		5	B/C	N/C	N/C	N/C	N/C
	2	3	BN/S	N/—	BN/—	N/—	N/—
		4	B/BC	N/—	BN/—	N/—	N/—
		5	BN/BC	N/—	BN/—	N/—	N/—
	3	3	BN/BC	N/—	BN/—	N/—	N/—
		4	B/B	N/—	BN/—	N/—	N/—
		5	BN/B	N/—	BN/—	N/—	N/—
	4	3	BN/B	BN/B	BN/—	N/—	N/—
		4	BN/B	BN/B	BN/B	N/—	N/—
		5	B/B	BN/B	BN/B	N/—	N/—
	5	3	BN/B	BN/B	BN/B	N/—	N/—
		4	BN/B	BN/B	BN/B	N/—	N/—
		5	BN/B	BN/B	BN/B	N/—	N/—
3	1	3	B/C	BC/S	BC/S	BC/S	BC/S
		4	B/C	BC/S	BC/S	BC/S	BC/S
		5	B/S	B/S	BC/S	B/S	B/S
	2	3	BC/S	BC/BC	BC/S	BC/BC	N/—
		4	B/BC	B/BC	B/BC	B/BC	N/—
		5	B/BC	B/BC	B/BC	B/BC	B/BC
	3	3	BC/BC	BN/B	BC/C	BN/B	BN/B
		4	B/B	BN/B	BN/—	BN/B	BN/B
		5	B/B	BN/B	BN/—	BN/B	BN/B
	4	3	B/B	BN/B	BN/B	BN/B	BN/B
		4	B/B	BN/B	BN/B	BN/B	BN/B
		5	B/B	BN/B	BN/B	BN/B	BN/B
	5	3	B/B	BN/B	BN/B	BN/B	BN/B
		4	B/B	BN/B	BN/B	BN/B	BN/B
		5	B/B	BN/B	BN/B	BN/B	BN/B
4	1	3	BC/S	BC/S	BC/S	BC/S	BC/S
		4	B/S	BC/S	BC/BC	BC/S	BC/S
		5	B/S	B/S	B/S	B/S	B/S
	2	3	BC/S	BC/BC	BC/BC	BC/BC	BC/BC
		4	B/S	BC/BC	BC/BC	BC/BC	BC/BC
		5	B/S	BC/BC	BC/BC	BC/BC	BC/BC
	3	3	B/B	BC/BC	BC/BC	BC/BC	BC/BC
		4	B/B	BC/BC	BC/BC	BC/BC	BC/BC
		5	B/B	B/BC	BC/BC	B/BC	B/BC
	4	3	B/B	BC/BC	BC/BC	BC/B	BC/B
		4	B/B	BC/B	BC/B	BC/B	BC/B
		5	B/B	BC/B	BC/B	BC/B	BC/B
	5	3	B/B	BC/B	BC/B	BC/B	BC/B
		4	B/B	BC/B	BC/B	BC/B	BC/B
		5	B/B	B/B	B/B	B/B	B/B
5	1	3	BC/S	BC/S	BC/S	BC/S	BC/S
		4	B/S	BC/S	BC/S	BC/S	BC/S
		5	B/S	B/S	B/S	B/S	B/S
	2	3	BC/S	BC/BC	BC/BC	BC/BC	BC/BC
		4	B/S	BC/BC	BC/BC	BC/BC	BC/BC
		5	B/S	B/BC	BC/BC	BC/BC	BC/BC
	3	3	B/B	BC/BC	BC/BC	BC/BC	BC/BC
		4	B/B	BC/BC	BC/BC	BC/BC	BC/BC
		5	B/B	B/BC	B/BC	B/BC	B/BC
	4	3	B/B	BC/B	BC/BC	BC/B	B/B
		4	B/B	B/B	B/B	B/B	B/B
		5	B/B	B/B	B/B	B/B	B/B
	5	3	B/B	BC/B	B/B	BC/B	BC/B
		4	B/B	B/B	B/B	B/B	B/B
		5	B/B	B/B	B/B	B/B	B/B

B = bearing; BC = bearing cleavage; BN = bearing net tension; C = cleavage; N = net tension; S = shear-out.

TABLE V
Bearing Strengths of [0/0/30/30] Specimens, MPA

			Preload moments				
W/D	*E/D*	*K/D*	0 Nm	2 Nm	3 Nm	4 Nm	5 Nm
2	1	3	129	220	241	203	246
		4	153	235	246	241	235
		5	158	264	243	245	265
	2	3	208	228	260	243	242
		4	218	260	259	285	245
		5	228	258	249	267	232
	3	3	214	282	278	276	234
		4	225	254	261	237	234
		5	210	284	263	250	244
	4	3	172	255	251	265	264
		4	212	258	228	240	257
		5	165	272	252	239	234
	5	3	187	256	287	269	250
		4	233	267	275	235	203
		5	196	248	259	257	245
3	1	3	185	280	309	323	300
		4	134	357	377	335	350
		5	161	293	302	290	335
	2	3	256	373	427	404	413
		4	260	342	421	395	379
		5	286	351	347	428	381
	3	3	295	444	471	424	391
		4	331	448	474	440	385
		5	319	461	415	421	401
	4	3	309	461	461	463	383
		4	327	441	496	440	410
		5	338	398	466	432	426
	5	3	220	402	482	449	433
		4	256	434	430	442	439
		5	346	492	490	437	431
4	1	3	135	202	253	245	319
		4	163	296	309	324	331
		5	167	284	306	330	359
	2	3	206	369	386	335	413
		4	229	416	411	386	395
		5	206	242	484	346	313
	3	3	265	443	484	450	487
		4	284	463	470	452	497
		5	303	521	497	498	479
	4	3	302	443	488	521	485
		4	268	513	539	512	508
		5	325	462	526	498	511
	5	3	303	468	512	473	475
		4	301	480	486	503	499
		5	338	530	554	511	535
5	1	3	164	253	293	292	323
		4	146	273	335	345	288
		5	165	299	371	312	339
	2	3	220	400	439	387	395
		4	201	435	410	412	445
		5	181	374	449	321	381
	3	3	266	478	505	454	515
		4	287	509	522	522	574
		5	273	510	509	543	510
	4	3	275	525	548	484	520
		4	285	505	550	571	535
		5	316	519	552	476	583
	5	3	269	484	555	513	554
		4	296	478	590	554	491
		5	329	479	554	536	550

TABLE VI
Bearing Strengths of [0/0/45/45] Specimens, MPA

			Preload moments				
W/D	*E/D*	*K/D*	0 Nm	2 Nm	3 Nm	4 Nm	5 Nm
2	1	3	159	234	262	232	217
		4	125	237	233	237	202
		5	147	229	243	206	220
	2	3	205	259	246	250	205
		4	194	254	250	264	186
		5	178	253	245	254	233
	3	3	170	250	238	239	224
		4	174	222	240	258	226
		5	214	252	225	234	235
	4	3	204	246	253	262	205
		4	199	246	257	243	236
		5	186	235	230	193	240
	5	3	187	257	231	250	260
		4	203	249	262	246	215
		5	193	233	210	240	246
3	1	3	149	246	296	307	242
		4	138	328	325	305	337
		5	149	278	326	272	285
	2	3	196	402	402	407	375
		4	178	419	431	413	340
		5	230	414	424	364	417
	3	3	266	395	425	387	390
		4	200	437	378	392	405
		5	276	372	373	375	372
	4	3	187	411	421	429	397
		4	222	417	406	430	376
		5	217	407	457	413	408
	5	3	231	391	459	427	332
		4	236	391	470	386	342
		5	244	426	428	413	413
4	1	3	158	254	346	289	273
		4	153	342	344	327	346
		5	150	316	341	346	296
	2	3	202	365	429	428	444
		4	187	411	445	456	451
		5	179	411	416	400	413
	3	3	217	441	540	473	429
		4	213	472	453	478	536
		5	263	476	503	478	494
	4	3	202	427	443	455	465
		4	246	454	541	491	476
		5	269	416	501	456	471
	5	3	203	512	521	478	485
		4	247	477	520	485	489
		5	199	512	518	481	444
5	1	3	141	247	273	270	287
		4	145	326	367	313	321
		5	172	290	349	283	302
	2	3	199	367	375	438	372
		4	223	345	425	432	456
		5	203	373	412	407	414
	3	3	202	457	529	504	440
		4	207	494	595	424	541
		5	262	446	539	499	498
	4	3	223	466	518	494	435
		4	233	433	533	543	515
		5	213	475	523	527	465
	5	3	201	473	553	503	494
		4	226	560	557	480	496
		5	228	497	549	496	560

joint does not carry any load from this moment, and any failure is not created in the outer hole. Briefly, net tension and cleavage modes are catastrophic and result from excessive tensile stresses, whereas the bearing mode is local and progressive damage and is related to compressive failure. Net tension, cleavage, and shear-out modes can be avoided by increases in end distance E and width W of the structural part for a given thickness; nonetheless, bearing damage cannot be avoided by any modification of the specimen geometry.[11–13] In fact, the failure modes change from cleavage or net tension to shear-out or bearing, depending on increasing W/D, E/D, and K/D ratios in this study. Meanwhile, the applied and/or increasing applied preload moments affect the production of failure modes without a doubt. For instance, when W/D was 2 for all E/D and K/D ratios, the failure modes were observed in the outer hole without preload moments (0 Nm), but after the application of various preload moments (2, 3, 4, and 5 Nm), failure was generally not observed in the outer hole. Additionally, when W/D was 4, E/D was 5, and K/D was 3, the failure mode was bearing/bearing without preload moments, although the mode changed to bearing cleavage/bearing after the preload moments were applied. On the other

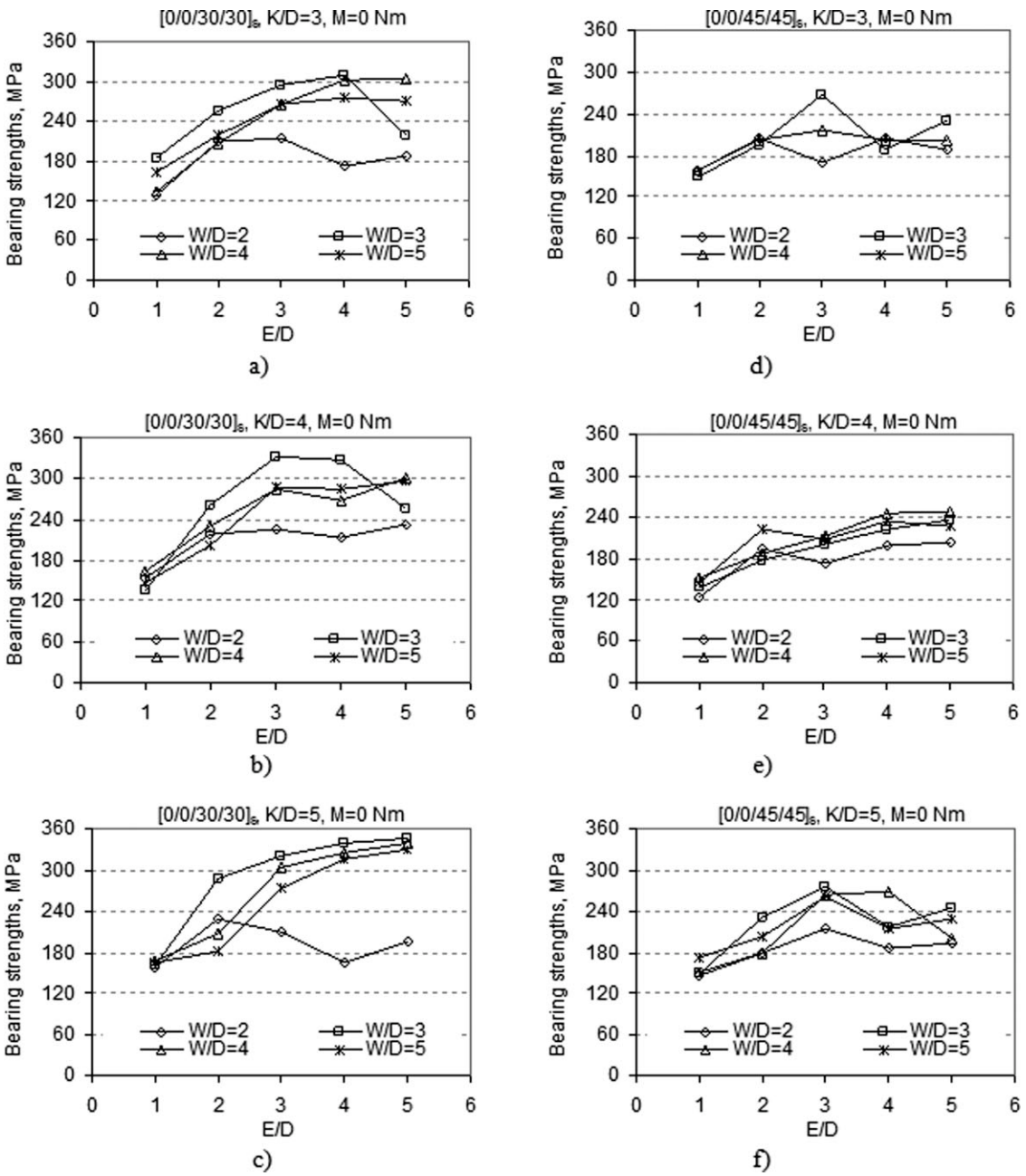

Figure 5 Effect of the E/D ratio on the bearing strength with respect to the W/D ratio.

hand, the applied preload moments caused catastrophic failure for a number of specimens with a mixed failure mode. According to Tables III and IV, the failure modes for $[0°/0°/30°/30°]_s$ and $[0°/0°/45°/45°]_s$ generally differed from each other for similar geometries. The amount of bearing failure modes was higher for $[0°/0°/30°/30°]_s$ specimens than for $[0°/0°/45°/45°]_s$ specimens. This is very important because the bearing failure mode is desirable in comparison with other failure modes for a safety design in real bolted-joint applications.

The average values of bearing strengths were calculated with the maximum failure loads of three similar specimens. The magnitudes of the bearing strengths for the tested $[0°/0°/30°/30°]_s$ and $[0°/0°/45°/45°]_s$ specimens are presented in Tables V and VI, respectively. These tables indicate that the bearing strengths increased with increasing W/D and E/D ratios generally, but it cannot be said that this result is valid for increasing K/D ratios. For instance, when W/D and E/D were 2 and K/D was 3, the bearing strengths were equal to 208 and 205 MPa, whereas when W/D, E/D, and K/D were 5, the values were 329 and 2228 MPa without a preload moment for the $[0°/0°/30°/30°]_s$ and $[0°/0°/45°/45°]_s$ specimens, respectively (Tables V and VI). In addition, bearing strengths without preload moments were calculated to be lower than the

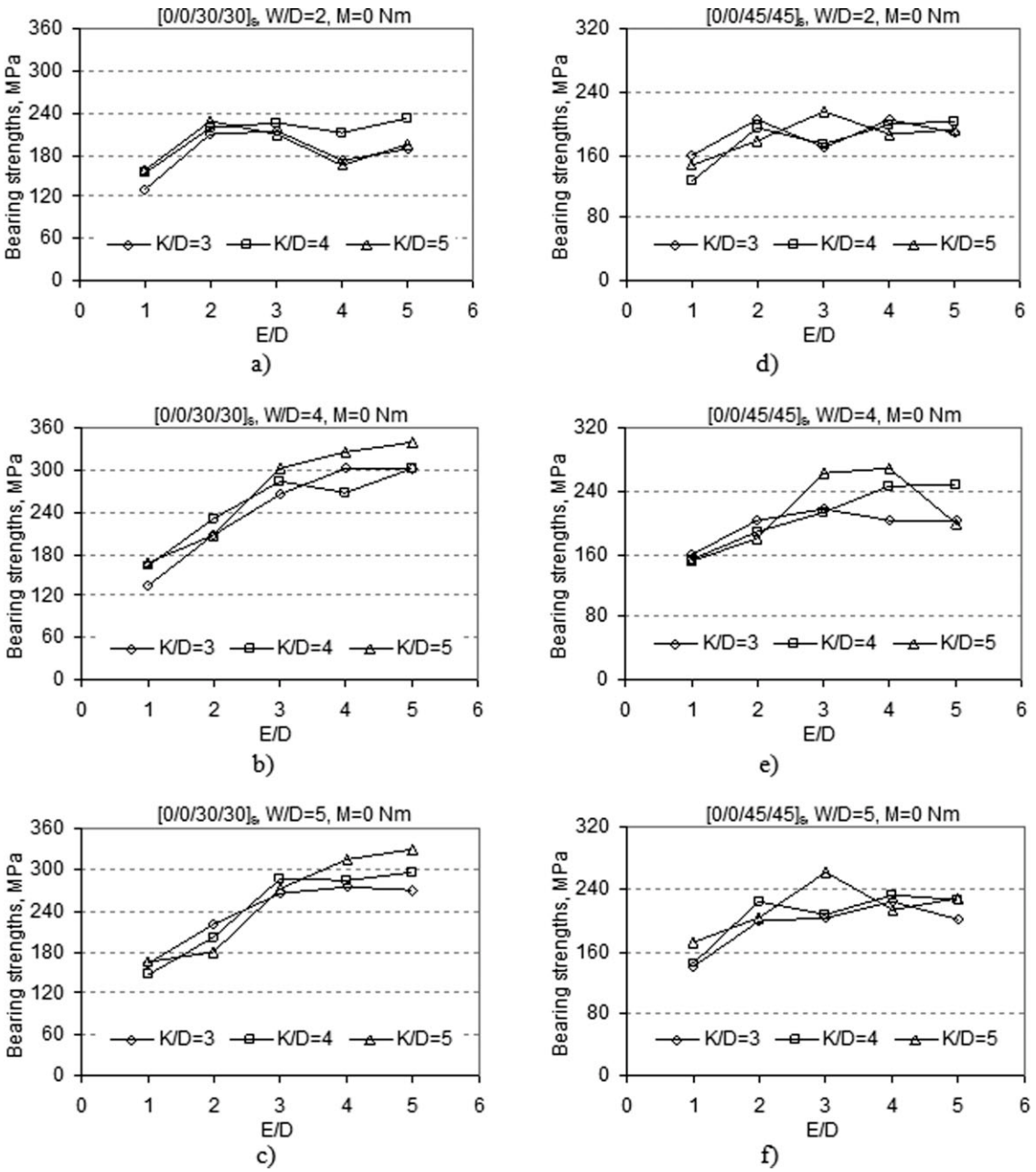

Figure 6 Effect of the E/D ratio on the bearing strength with respect to the K/D ratio.

applied preload moments. For example, when W/D, E/D, and K/D were 4, the bearing strength without a preload moment was 268 MPa; nevertheless, it was calculated to be 513 MPa under an applied preload moment of 2 Nm for the $[0°/0°/30°/30°]_s$ specimen (Table V). Similarly, it was determined to be 246 MPa without a preload moment and 454 MPa under an applied preload moment of 2 Nm for the $[0°/0°/45°/45°]_s$ specimens (Table VI). Applying the preload moments clearly led to higher bearing strength values because pressure was applied to the composite specimen by washers. Additionally, some tensile load was carried by the washers. In other words, the negative effects of the existence of bolt holes were reduced by the washers. Consequently, the bearing strengths under applied preload moments were higher than those without any preload moments.

The effect of the E/D ratio on the bearing strength is shown in Figures 5–7 for some tested specimens ($[0°/0°/30°/30°]_s$ and $[0°/0°/45°/45°]_s$ specimens) with respect to W/D and K/D ratios and applied preload moments. These figures show that the bearing strengths generally increased with increasing E/D ratios. Nevertheless, this increase was not linear because various unwanted conditions could occur through the production or preparation process of the

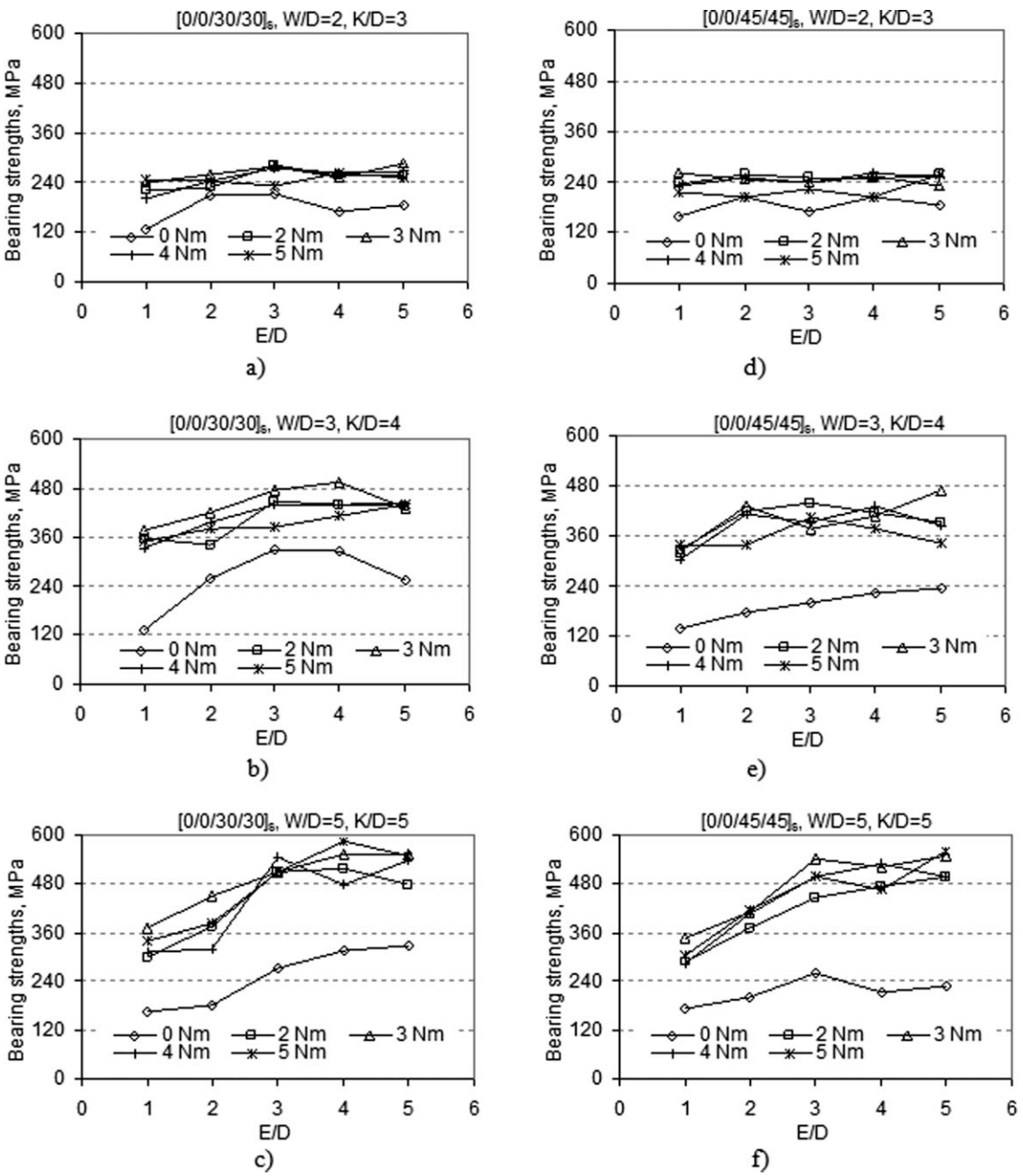

Figure 7 Effect of the E/D ratio on the bearing strength with respect to the applied preload moments.

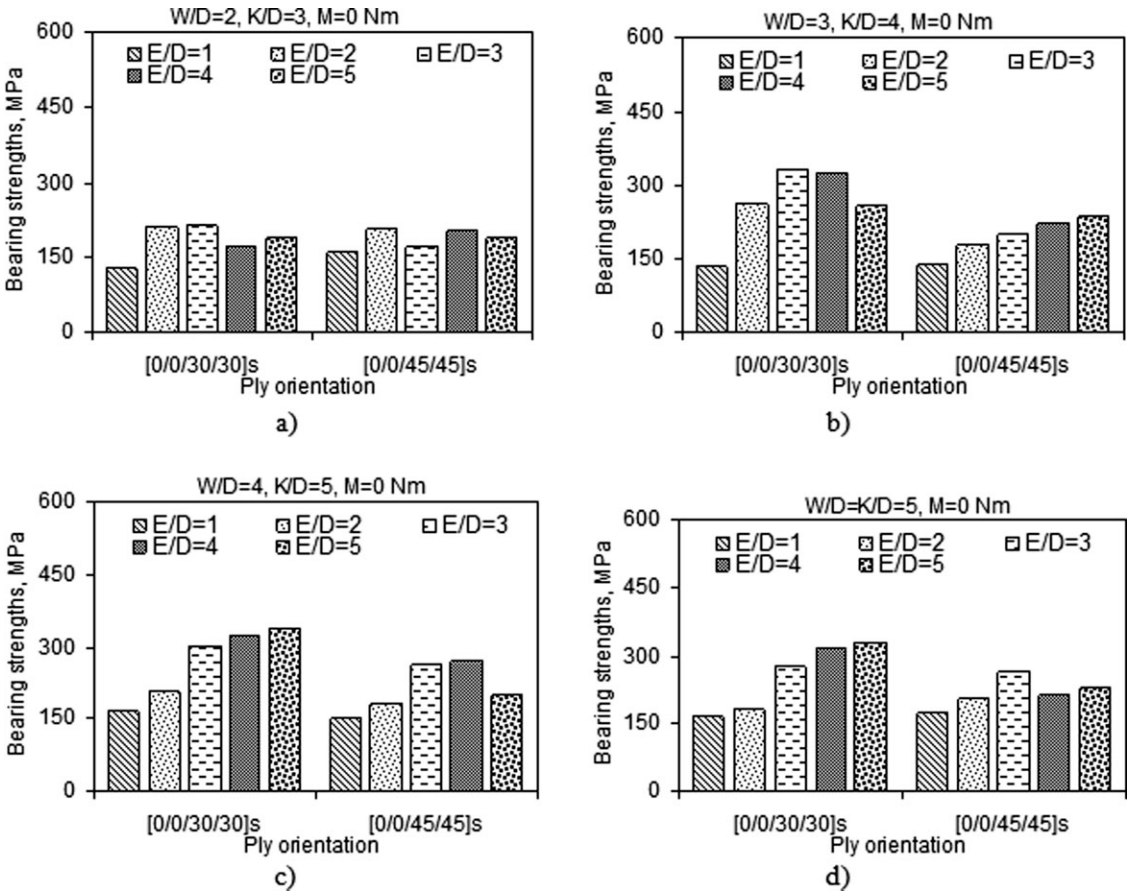

Figure 8 Effect of the ply orientation on the bearing strength with respect to the E/D ratio.

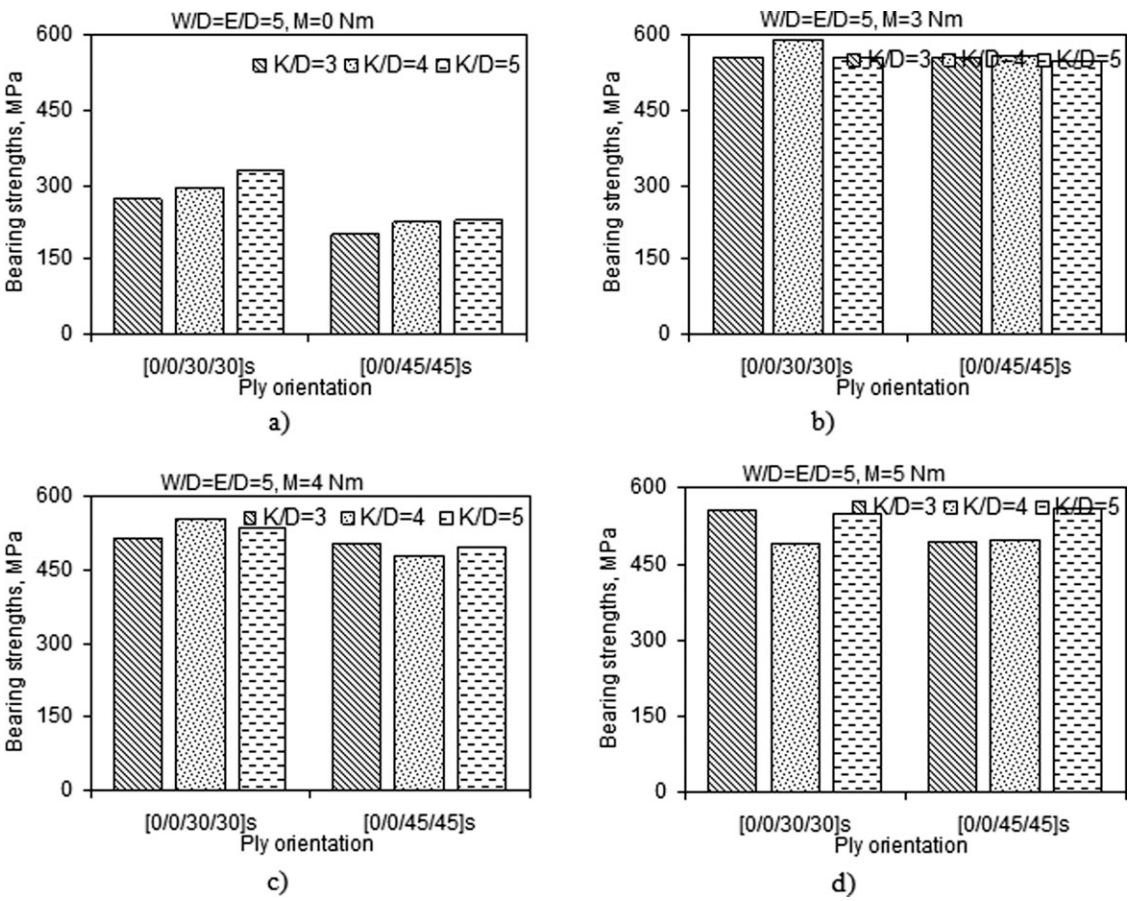

Figure 9 Effect of the ply orientation on the bearing strength with respect to the K/D ratio.

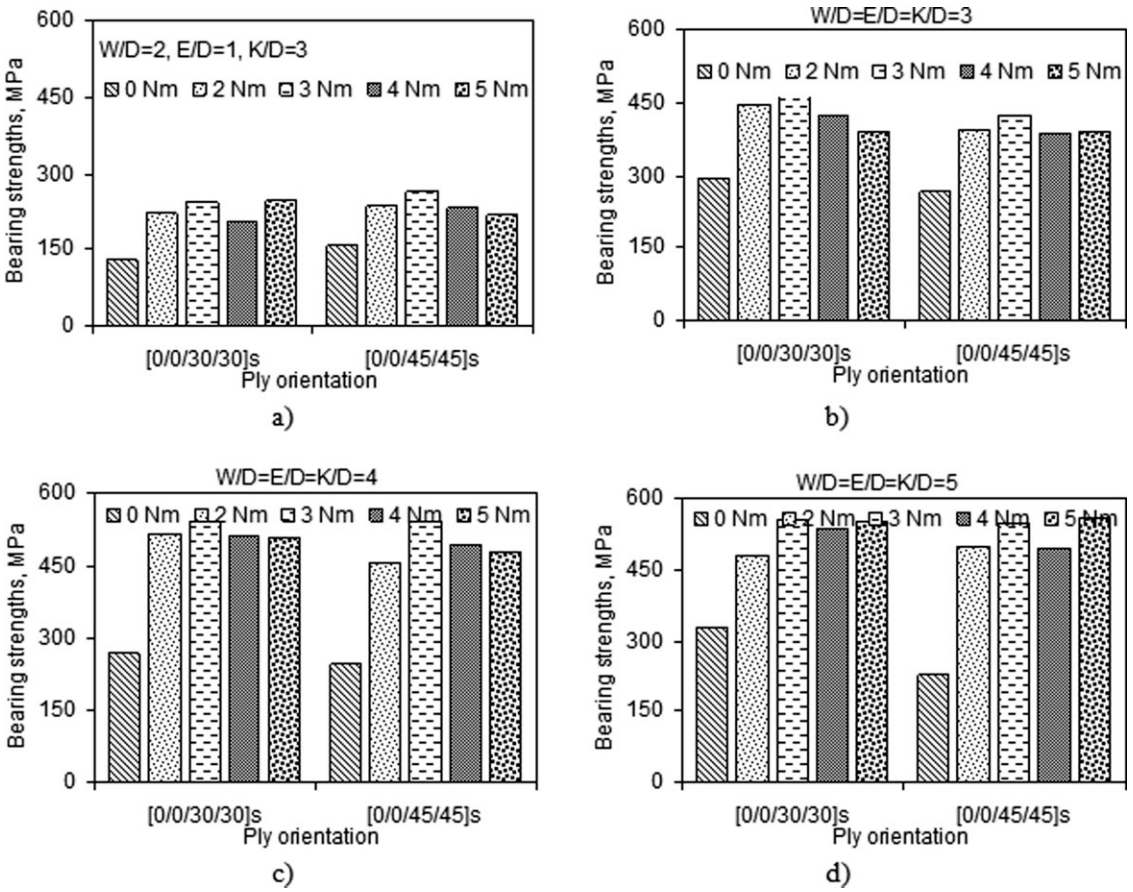

Figure 10 Effect of the ply orientation on the bearing strength with respect to the applied preload moments.

specimens, such as porosity and microcracking of the fibers and/or matrix. Meanwhile, when E/D was 1, the bearing strength was obviously smaller than that at other E/D ratios. On the other hand, the weakest geometrical parameters were observed at $E/D = 1$. Moreover, the other weakest geometrical parameter was seen at $W/D = 2$, as shown in Figure 5. When W/D was 2, the bearing strength was generally smaller than at other W/D ratios. Additionally, the bearing strength increased with increasing K/D ratio (Fig. 6). For a two-serial-bolted joint, the weakest K/D ratio was observed to be 3. The minimum ratio had to be selected to be 3 because of the diameter of the washers (15 mm). According to Figure 7, the bearing strengths without preload moments were clearly lower than those with applied preload moments. It has been said that applied preload moments are suitable with high bearing strengths. This means that the load capacity of a two-serial-bolted composite joint under applied moments is higher than that without applied preload moments.

The effects of selected ply orientations on the bearing strengths for some tested specimens related to the E/D and K/D ratios and applied preload moments are illustrated in Figures 8–10, respectively. These figures also point out the bearing strengths generally increased with increasing E/D and K/D ratios and applied preload moments. Furthermore, the bearing strengths of $[0^\circ/0^\circ/30^\circ/30^\circ]_s$ specimens were frequently higher than those of $[0^\circ/0^\circ/45^\circ/45^\circ]_s$ specimens. In other words, $[0^\circ/0^\circ/30^\circ/30^\circ]_s$ oriented specimens were stronger than $[0^\circ/0^\circ/45^\circ/45^\circ]_s$ oriented specimens on the basis of the calculated bearing strengths. Meanwhile, Figure 10 shows that the magnitude of the applied preload moment was enough if it was chosen to be 3 Nm for both $[0^\circ/0^\circ/30^\circ/30^\circ]_s$ and $[0^\circ/0^\circ/45^\circ/45^\circ]_s$ specimens. The bearing strengths for an applied preload moment of 2 Nm and without a preload moment were smaller than those with an applied preload moment of 3 Nm. However, the magnitudes of the bearing strengths decreased when the applied preload moments were 4 or 5 Nm. Therefore, it is understood that the highest values of the preload moments (4 or 5 Nm) may have caused crushing and/or microcracking in the glass fibers and/or epoxy matrix of the composite plates.

CONCLUSIONS

An experimental failure analysis was performed to determine the failure behavior of two-serial-bolted

composite laminates with various applied preload moments and without preload moments. The geometrical parameters defined E/D, W/D, and K/D ratios and material parameters in terms of the orientations of the laminated composite plates as $[0°/0°/30°/30°]_s$ and $[0°/0°/45°/45°]_s$ were considered. One of the parameters was changed, whereas the others were held constant for the duration of the tests. According to current experimental analysis results, some important remarks can be made in a few words. First, some geometrical parameters could not be used, such as $E/D = 1$ or 2, $W/D = 2$, and $K/D = 3$, because of the load-carrying capacity and the occurrence of failure modes. The bearing strengths for these ratios were generally lower than those for other selected ratios. Second, the bearing strengths of the specimens under various preload moments were higher than those without preload moments. In other words, increasing the preload moments was very suitable for a safe two-serial-bolted joint configuration because of the provided bearing mode and high values of the bearing strength, in that bearing failure was more advantageous than cleavage, net tension, or shear-out failure from a safe design. Additionally, the magnitude of the preload moment was appropriate when it was 3 Nm. Finally, $[0°/0°/30°/30°]_s$ stacked plates were stronger than $[0°/0°/45°/45°]_s$ stacked plates among the tested composite plates.

The authors thank the personnel of Izoreel Firm (Izmir, Turkey) and Murat Eroglu in particular for their endless effort during the manufacturing of the composite plates and preparation of the test specimens.

References

1. Choi, J.-H.; Chun, Y-J. J Compos Mater 2003, 37, 2163.
2. Wu, T. J.; Hahn, H. T. Compos Sci Technol 1997, 58, 1519.
3. Scalea, F. L. D.; Cappello, F.; Cloud, G. L. J Thermoplast Compos Mater 1999, 12, 13.
4. Whitworth, H. A.; Aluko, O.; Tomlinson, N. A. Eng Fract Mech 2008, 75, 1829.
5. Dano, M. L.; Kamal, E.; Gendron, G. Compos Struct 2007, 79, 562.
6. Pierron, F.; Cerisier, F.; Grediac, M. J Compos Mater 2000, 34, 1028.
7. Madenci, E.; Shkarayev, S.; Sergeev, B.; Oplinger, D. W.; Shyprykevich, P. Int J Solids Struct 1998, 35, 1793.
8. McCarthy, C. T.; McCarthy, M. A.; Lawlor, V. P. Compos B 2005, 36, 290.
9. Yan, Y.; Wen, W. D.; Chang, F. K.; Shyprykevich, P. Compos A 1999, 30, 1215.
10. Tong, L. Compos A 2000, 31, 609.
11. Lin, C. C.; Lin, C. H. Int J Solids Struct 1999, 36, 763.
12. Meola, C.; Squillace, A.; Giorleo, G.; Nele, L. J Compos Mater 2003, 37, 1543.
13. Okutan, B. Compos B 2002, 33, 567.
14. Chang, F. K.; Scott, R. A.; Springer, G. S. J Compos Mater 1982, 16, 470.
15. Pakdil, M.; Sen, F.; Sayman, O.; Benli, S. J Reinforced Plast Compos 2007, 26, 1239.
16. Sayman, O.; Siyahkoc, R.; Sen, F.; Ozcan, R. J Reinforced Plast Compos 2007, 26, 1051.
17. Mallick, P. K. Fiber-Reinforced Composites Materials, Manufacturing, and Design, 2nd ed.; Marcel Decker: New York, 1993.
18. Jones, R. M. Mechanics of Composite Material; Taylor & Francis: Washington, DC, 1999.
19. Gibson, R. F. Principals of Composite Material Mechanics; McGraw-Hill: New York, 1994.
20. Sen, F. Ph.D. Thesis, Dokuz Eylül University, 2007.
21. Reddy, J. N. Mechanics of Laminated Composite Plates: Theory and Analysis; CRC: Boca Raton, FL, 1997.
22. Kradinov, V.; Madenci, E.; Ambur, D. R. Compos Struct 2007, 77, 127.